

Corrosion analysis and models for some composites behavior in saline media

Alina Barbulescu and Lucica Orac

Abstract— Corrosion is one of the main causes of metals degradation, which consists of superficial and structural changes. It causes damages and economic loss and can be prevented mainly by choosing the materials with the best properties for the working conditions.

When a material is introduced in an aqueous medium, an electrochemical attack is produced. It can be combined with other effects, as, for example, that of cavitation.

In this context, we present the results of our corrosion experiments on some composites materials (simple and oil - impregnated) introduced in saline water and in a cavitation field produced by ultrasounds, in an experimental set - up especially build for this purpose.

Also, mathematical models of absolute mass loss in time and on surface for each material are given and comparisons with other copper – base alloys are done.

Keywords—corrosion, cavitation, composites, mass loss

I. INTRODUCTION

Corrosion is the phenomenon of spontaneous destruction of metallic surfaces or alloys under the action of the medium factors, as gasses, electrolytic solutions, microorganisms. The electrochemical corrosion appears in the presence of electrolytic solution. If a cavitation field is also present, the electrochemical corrosion is combined with the erosion process. In marine submerged areas, the seawater is the electrolyte; in marine atmospheric areas, salt spray provides the electrolyte.

The corrosion study needs chemical, physical, metallurgical and mechanical perspectives, as well as environmental aspects.

As the corrosion – erosion can dramatically affects the functioning of different machine components, the use of some resistant materials to design them, is a solution.

Due to their resistance in saline media many copper base alloys are used in naval constructions. [1]

In the last years, the composites use is increasing, taking

Manuscript received December 3, 2008; Revised version received 2008. This work was supported by CNCIS under Grant 902/2007.

Alina Barbulescu is with the Ovidius University of Constanta, Faculty of Mathematics and Computers Science, Bd. Mamaia, 124, 900527, Constanta, ROMANIA (corresponding author to provide phone: 0040-722-542353; e-mail: alinadumitriu@yahoo.com).

Lucica Orac is with Dunarea de Jos University of Galati, Faculty of Metallurgy and Materials Science, Str. Domneasca, 111, Galati, ROMANIA (e-mail: lucia_orac@yahoo.com).

account of their anticorrosive properties. [2] - [3]

In this study we focused on the analysis of some composite materials, in saline media and in cavitation field.

The base material was obtained by 87 % Cu, 7% Sn, 4% Zn, 2% Pb powder (sample 1). These powders were sintering with graphite in different proportions (the samples 3 and 5) and half of them were oil - impregnated at high temperature (the samples 2, 4 and 6). The graphite's percentage is presented in Table I.

Table I. Composite' s graphite percentage

SAMPLE	COMPOSITION
1	0 % graphite
2	0 % graphite, impregnated
3	1.5 % graphite
4	1.5 % graphite, impregnated
5	2.5 % graphite
6	2.5 % graphite, impregnated

II. MATERIALS ANALYSIS AND EXPERIMENTAL METHODS

It is assumed that in the simplest case on a corroding metal electrode, two electrochemical reactions may proceed:

- ionization of metal atoms, together with the reverse reaction;

- cathodic depolarization, i.e. reduction of oxidant present in solution to reduced form, together with the reverse reaction.

The polarization current of such a corrosion system is the sum of partial current of reactions. [4]

The corrosion stage of a material can be observed by:

- qualitative methods, as microscopic observations;
- quantitative methods, as corrosion speed calculation.

Some methods of corrosion parameters determination can be mentioned: gravimetric, galvanostatic and potentiostatic methods.

In our experiments, both types of methods - quantitative methods and qualitative - were applied.

At the beginning, the materials were analyzed using an optical microscope and a scanning electron microscope (SEM).

The optical microscope, called also light microscope, uses the light and a lens system to increase the samples images.

SEM is a type of electron microscope that images the sample surface by scanning it with a high-energy beam of electrons in a raster scan pattern. The electrons interact with

the atoms that make up the sample producing signals that contain information about the sample's surface topography, composition and other properties such as electrical conductivity [5].

The observation was repeated at the experiments end.

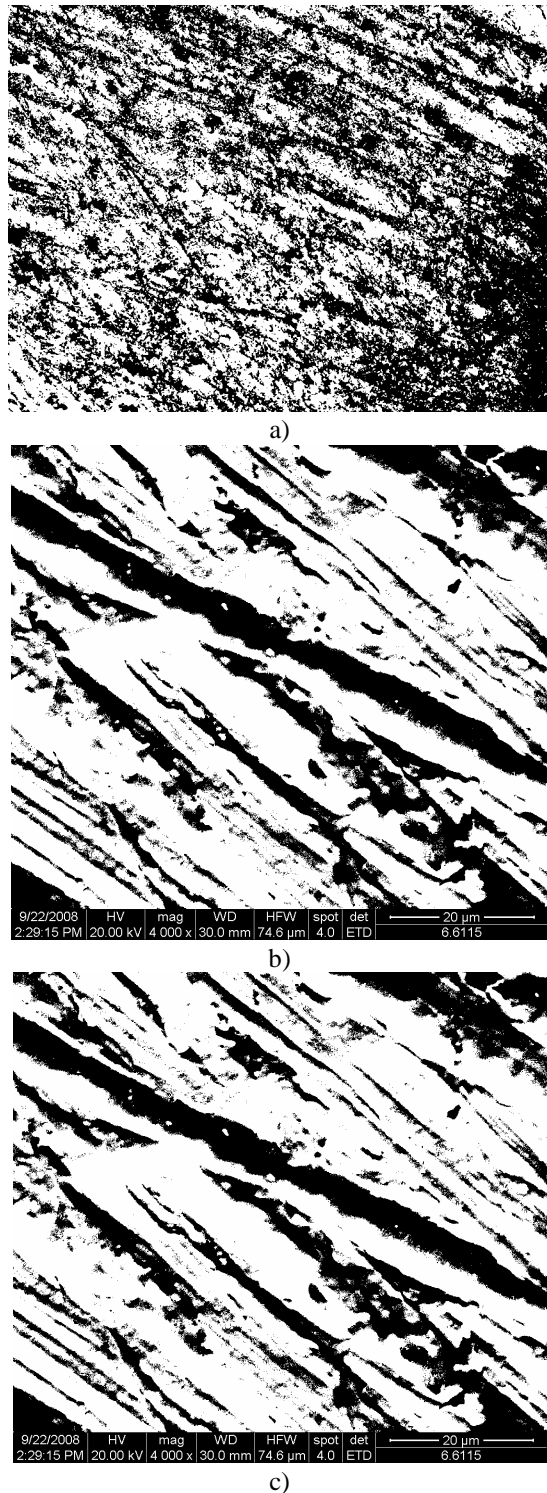


Fig.1. a) Image of sample 5 before the experiment (light microscope -100x)
 b) Image of sample 5 before the experiment (SEM - 4000x);
 c) Image of sample 5 after the erosion – corrosion experiment

(SEM - 4000x)

In Fig.1, the microstructures of some samples of material 5, at the optical microscope with magnification x100, respectively at SEM, with magnification x4000 are presented.

A. Electrochemical methods

Different methods can be applied to determine the material resistance [6] – [7].

The electrochemical methods are used for different purposes [8], for example to evaluate the metal corrosion rate in electrolytic environment in a very wide range of values from $\mu\text{A}/\text{cm}^2$ to A/cm^2 , equivalent to a linear corrosion rate from fractions of $\mu\text{m}/\text{year}$ to several mm/year [4] .

In this case, the galvanostatic method was applied in order to determine the corrosion parameters (current density, potential, corrosion speed and wear speed).

The experiments were carried out using a conventional three electrode cell having as the working electrode a composite sample with a surface of 1 cm^2 . Prior to the experiments the electrode was cleaned and polished, wiped washed with acetone and finally with distilled water.

The counter electrode consisted of a piece of platinum wire.

The reference electrode to which all potentials are referred was the saturated Ag/AgCl electrode isolated from the main cell by a Hager - Luggin capillary.

The measurements were carried out at the room temperature, on a Voltalab 21 system connected to a PC. The software used was VoltaMaster 4. [9]

The working media consisted of a solution of 0.5M NaCl in distilled water.

For each sample the following tests sequence was performed:

- open circuit potential;
- general corrosion (to determine the polarization resistance);
- cyclic voltammetry;
- linear potential (to determine the Tafel curves);
- pitting voltage measurement.

B. The erosion – corrosion study in cavitation field

Cavitation is a physical phenomenon consisting of the creation in a liquid of very small vacuum bubbles, filled to a certain degree with vapours, gas or a mixture thereof, which under certain conditions implode. The implosion releases energy that can dislodge particles of materials exposed to the field action. [10]

The use of ultrasound power is becoming more widespread in both research and industrial context. Frequently, the applications being considered are driven by the associated phenomenon of acoustic cavitation. [11]

Acoustic cavitation may be briefly described as the inception, grows and oscillation of vapours or gas bubbles in a medium under the influence of ultrasound [12] - [14], giving rise to a range of physical, chemical and biological effects [15] - [17]. Erosion and unpassivation of solid boundary surfaces are phenomena of undisputable technical significance. [18]

The experiments were carried out in stationary saline water in cavitation field produced in an experimental set - up (Fig.2) especially built for this purpose that can also be used to study the corrosion – erosion in circulating media. It mainly consists of a tank for liquids, containing a transducer connected to a high frequency generator that excites the transducer to produce ultrasounds [19] – [21].

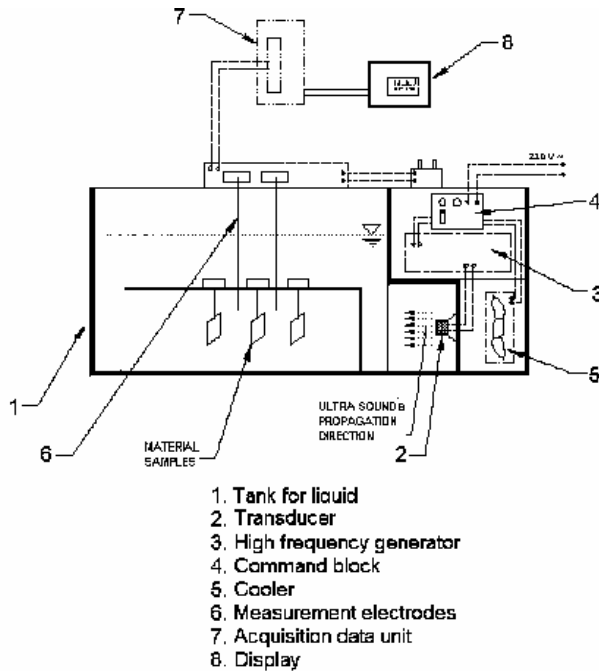


Fig.2. Experimental set - up

The cavitation was produced by the ultrasound field generated by the transducer module.

The study of the electrical signal induced at the boundary of cavitation field can be also done, by a variety of methods [20] – [23].

The tests were carried out at different powers at which the ultrasound generator works: 80 W, 120 W and 180 W. In what follows we shall present only the results obtained at 80 W.

As temperature determines a shift in the position of erosion zone, this parameter was kept constant at +21°C.

The test samples were machined to suitable dimensions, after which the surfaces exposed to cavitation were ground and polished. They were stored in a desiccator between the experiments.

The samples were put on the cavitation field 24 hours, by-stages of 30 minutes. Before and after each test, they were dried and weighed. The average mass loss was used to determine the erosion - corrosion rate.

III. RESULTS OF ELECTROCHEMICAL EXPERIMENTS

In this section we present only the experiments results concerning the samples 5 and 6.

The first step in the electrochemical analysis was to run an Open Circuit Potential experiment with duration of at least 30 minutes and a scan rate of 0.6s.

In Figs.3 and 4, the results of this test are given.

It can be seen that in the first case, after a sudden decreasing of potential, it tends to become stable at -283 mV; in the second case, a slow decreasing of the potential was registered, in the first 20 minutes.

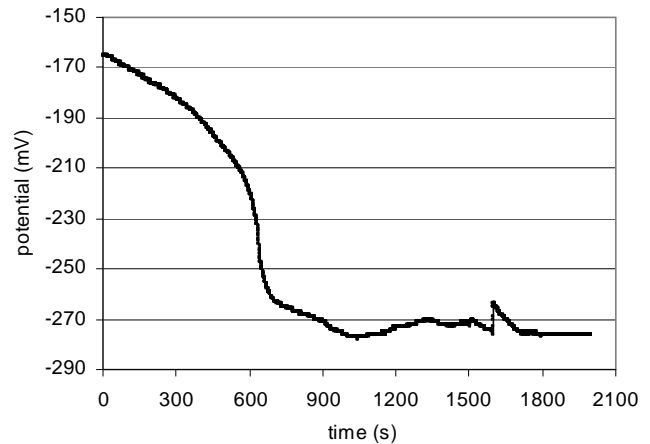


Fig.3. OCP graph – sample 5

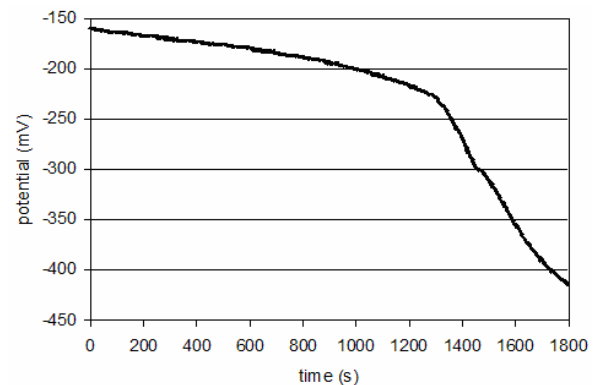


Fig.4. OCP graph – sample 6

It is known that thermodynamically, the less negative the OCP, the more sensitive to corrosion the sample is.

General corrosion test with VoltaMaster4 automatic calculates the polarization resistance (R_p) determined from cyclic or linear voltammetries.

$\text{Cu}^{2+}/\text{Cu}^+$ and Cu^+/Cu^0 reduction processes can not be observed from the cyclic voltammetries (Figs. 5 and 6).

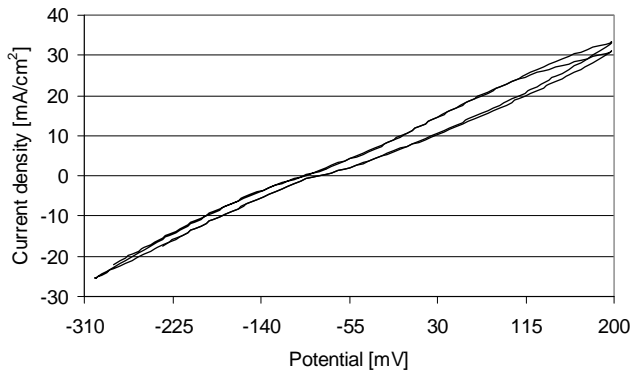


Fig.5. The voltammogram of sample 5

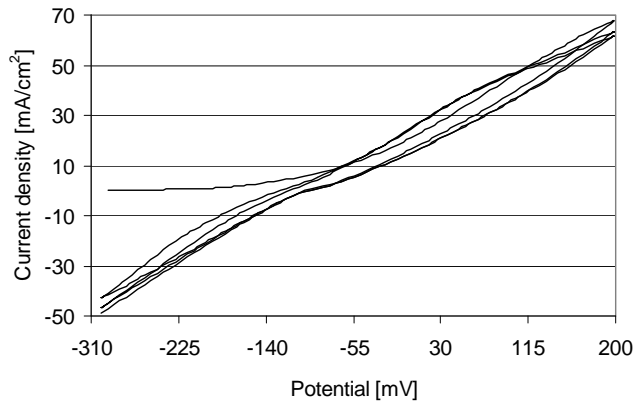


Fig.6. The voltammogram of sample 6

The linear voltammetries were performed around the rest potential. In our case, 7 individual linear voltammetries were recorded at a scan rate of 2mV/s. In their graphs (Figs. 7 and 8) the black lines represent the polarization resistance and the grey ones, the corrosion potential measurements versus time of all voltammetries.

The recorded mean polarization resistance was respectively $660.646 \text{ ohm} \cdot \text{cm}^2$ and $784.393 \text{ ohm} \cdot \text{cm}^2$.

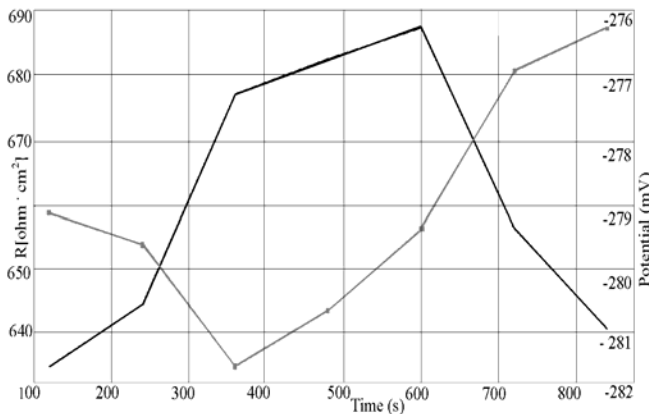


Fig.7. The polarization resistance and the corrosion potential – sample 5

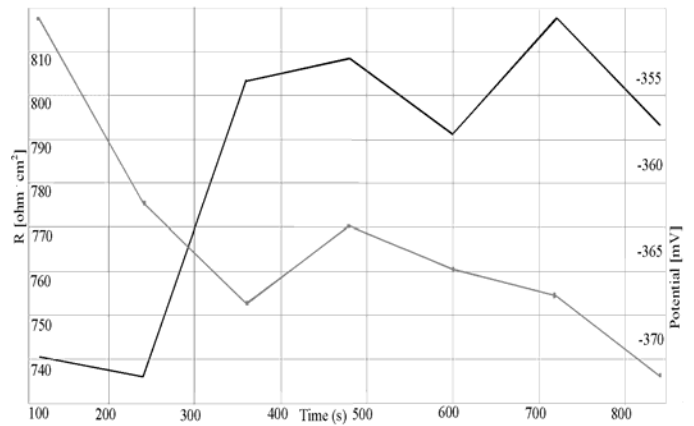


Fig.8. The polarization resistance and the corrosion potential – sample 6

The recorded mean potential was -279.549 mV , respectively -364.44 mV .

The determination of corrosion current regularly present at the surface of a metal which is in contact with a corroding solution was made using the Tafel equation. The study was made in an interval of $\pm 1000 \text{ mV}$ (Fig.9) and $\pm 40 \text{ mV}$ (Fig.10) around the mean potentials, calculated at the previous step.

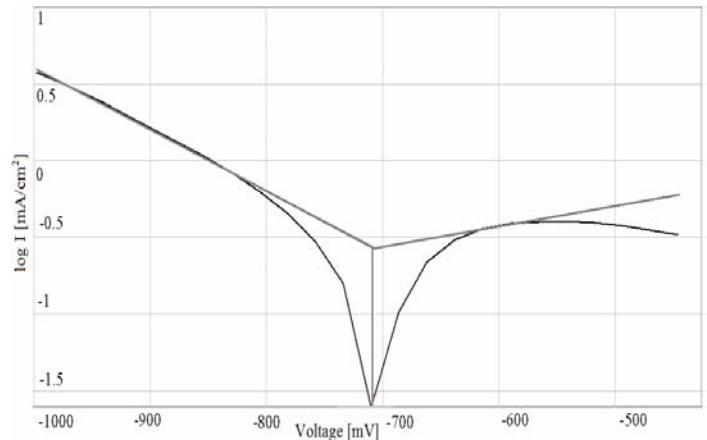


Fig.9. Polarization curves (Tafel) - sample 5

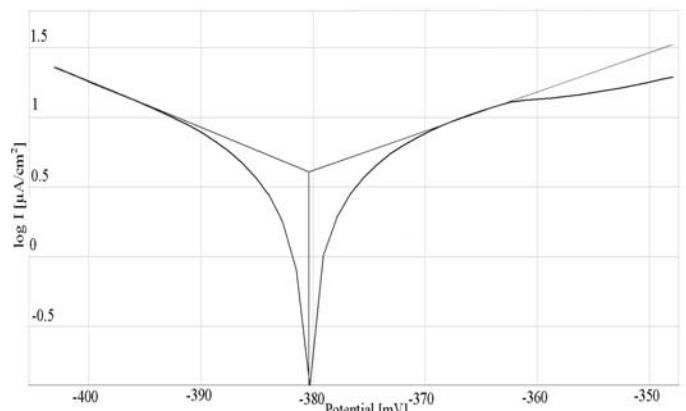


Fig.10. Polarization curves (Tafel) - sample 6

The results were:

- for an interval of ± 1000 mV around the mean potential calculated at the previous step, the corrosion potential of sample 5 was -707.2 mV and the corresponding current density, 0.3294mA/cm². The values corresponding to the sample 6 were respectively: -717 mV and 0.1404 mA/cm²;
- for an interval of ± 40 mV around the mean potential calculated at the previous step, the corrosion potential of sample 6 was -380.4 mV and the corresponding current density, 4.0576 μ A/cm².

For the pitting corrosion test, the work electrode was polarised at -10 mV versus the REF potential and this potential was scanned towards anodic polarisation at a scan rate of 1 mV/s with potential steps of 2.5 mV and 2.5 second duration. The current was measured.

The more anodic the "pitting potential", the less subject to pitting the sample is [10].

The tests results prove that all studied materials have been pasivated. For the samples 5 and 6, the critical pitting potential was respectively -63.8mV and -99.6mV.

IV. MATHEMATICAL MODELS

Using the experimental data, the mass loss equations in time were determined. They are respectively:

$$m_t = 1.241 + 1.97 \cdot 10^{-5}t - 8.36 \cdot 10^{-8}t^2 + 1.16 \cdot 10^{-10}t^3 - 5.08 \cdot 10^{-14}t^4, \tag{1}$$

$$m_t = 1.352 + 1.155 \cdot 10^{-6}t - 6.05 \cdot 10^{-9}t^2 + 8.52 \cdot 10^{-12}t^3 - 4.23 \cdot 10^{-15}t^4, \tag{2}$$

$$m_t = 1.761 - 9.342 \cdot 10^{-8}t + 3.462 \cdot 10^{-10}t^2 + 9.964 \cdot 10^{-13}t^3 - 1.52 \cdot 10^{-15}t^4, \tag{3}$$

$$m_t = 1.207 + 1.467 \cdot 10^{-7}t + 3.146 \cdot 10^{-9}t^2 - 4.48 \cdot 10^{-12}t^3 + 1.2 \cdot 10^{-15}t^4 \tag{4}$$

$$m_t = 2.859 - 5.1 \cdot 10^{-6}t + 1.176 \cdot 10^{-8}t^2 - 9.625 \cdot 10^{-12}t^3 + 1.514 \cdot 10^{-15}t^4, \tag{5}$$

$$m_t = 1.291 + 2.97 \cdot 10^{-6}t - 1.45 \cdot 10^{-8}t^2 + 2.30 \cdot 10^{-11}t^3 - 1.16 \cdot 10^{-14}t^4. \tag{6}$$

where t is the time and m_t is the mass at the moment t .

So, the mass variation models of all composites samples are described by polynomial functions of fourth degree, of the type:

$$m_t = a_0 + a_1t + a_2t^2 + a_3t^3 + a_4t^4 + \varepsilon_t,$$

where ε_t is the residual.

The curves' allures are presented in Figs. 11 – 16.

In order to validate the models the first step is to verify if the coefficients are significant, at a significance level of 5%.

Point of view of statistics it means that the following hypotheses must be tested:

$$H_0: \text{the coefficient is null}$$

and

$$H_0: \text{the ensemble of coefficients is significant.}$$

It can be done using t and F tests.

Let us denote by:

- n - the sample volume (48, in our case),
- k - the number of estimated coefficients (5, in our case),
- \hat{a}_i - the calculated coefficients ($i=1, \dots, 5$, in our case),
- $\hat{\sigma}_{\hat{a}_i}$ - the mean square deviation of \hat{a}_i ,

$$\hat{A} = \begin{pmatrix} \hat{a}_0 \\ \hat{a}_1 \\ \hat{a}_2 \\ \hat{a}_3 \\ \hat{a}_4 \end{pmatrix} \text{ - the vector that contains the calculated coefficients,}$$

coefficients,

- α - the significance level (5%, in this case),
- $t_{\alpha/2, n-k-1}$ - the tabled critical value of Student distribution with $n-k-1$ degrees of freedom, at the significance level α ,
- $F_{\alpha, k, n-k-1}$ - the tabled critical value of Fisher distribution with k and $n-k-1$ degrees of freedom, at the significance level α ,
- $\hat{\Omega}_{\hat{a}}$ - the variance - covariance matrix.

t test: If

$$\left| \frac{\hat{a}_i}{\hat{\sigma}_{\hat{a}_i}} \right| \geq t_{\alpha/2, n-k-1},$$

we reject the hypothesis H_0 , at the significance level, α so \hat{a}_i is significantly not null.

F test: If

$$\frac{1}{q} \cdot A^t \cdot \hat{\Omega}_{\hat{a}}^{-1} \cdot A \geq F_{\alpha, k, n-k-1}$$

we reject hypothesis H_0 , at the significance level α , so the model is entirely significant. [24]

The tests t and F applied to the models (1) – (6) lead us to accept the hypotheses that the coefficients are not zero and the models are entirely significant.

The standard deviation, S , is very small (between 0.00026273 and 0.00130012) and the correlation coefficient, r , is close to 1 (between 0.94994379 and 0.974297). For each model, they are listed on the top, right hand side of the graphs.

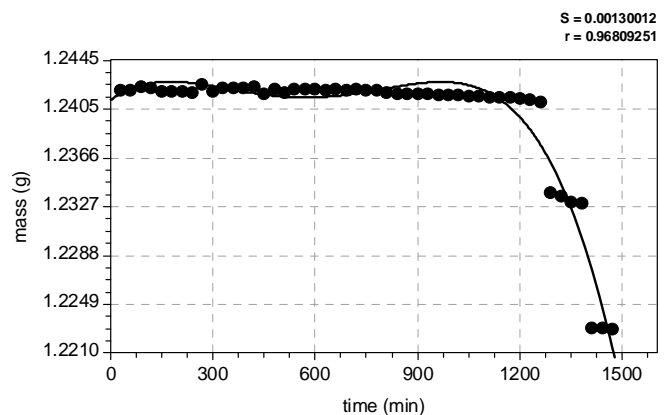


Fig.11. The graph of sample 1 mass variation

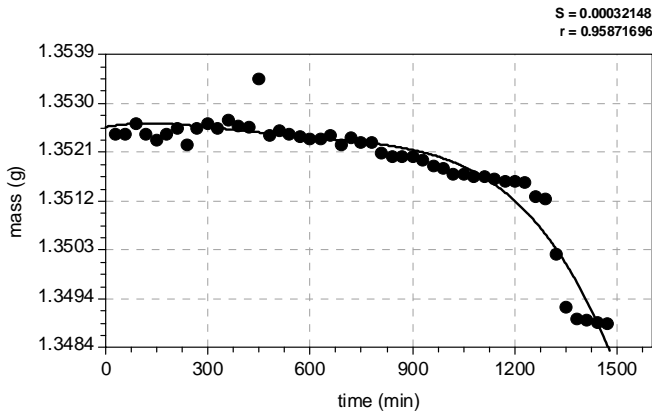


Fig.12. The graph of sample 2 mass variation

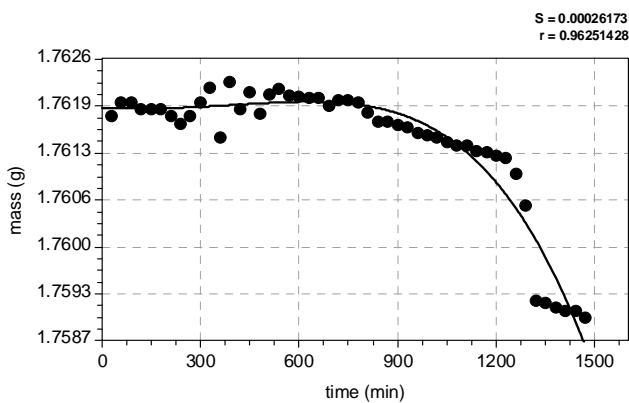


Fig.13. The graph of sample 3 mass variation

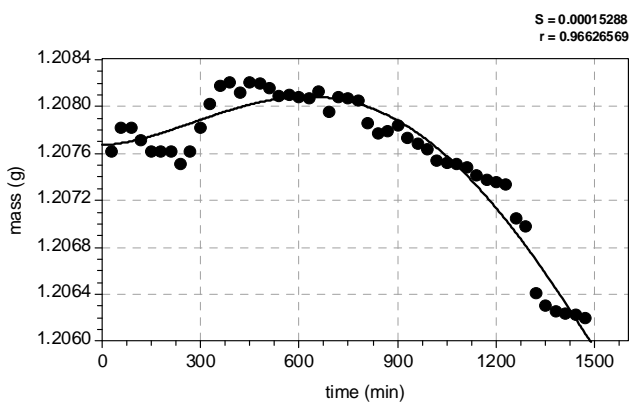


Fig.14. The graph of sample 4 mass variation

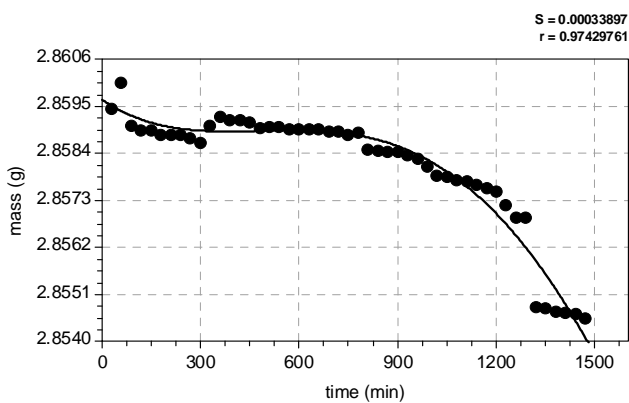


Fig.15. The graph of sample 5 mass variation

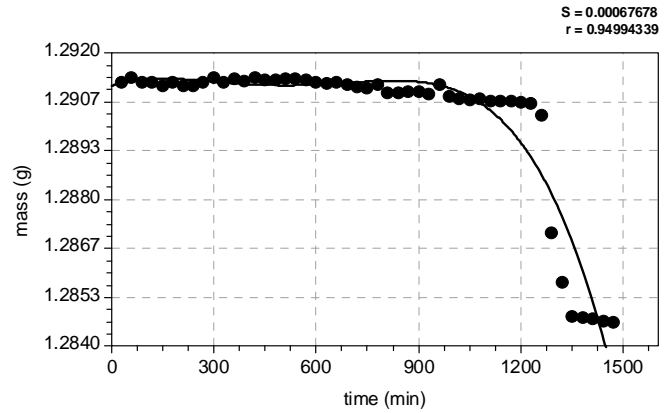


Fig.16. The graph of sample 6 mass variation

The graphs of errors from the models (1) – (6) are plotted in Figs. 17 - 22.

The second step in the models' validation is the residuals analysis.

The residuals are tested for normality (Jarque - Bera test, histogram and Q-Q plot), correlation (autocorrelation function analysis) and homoscedasticity (Bartlett test). [24]

To understand the results briefly theoretical presentation is necessary.

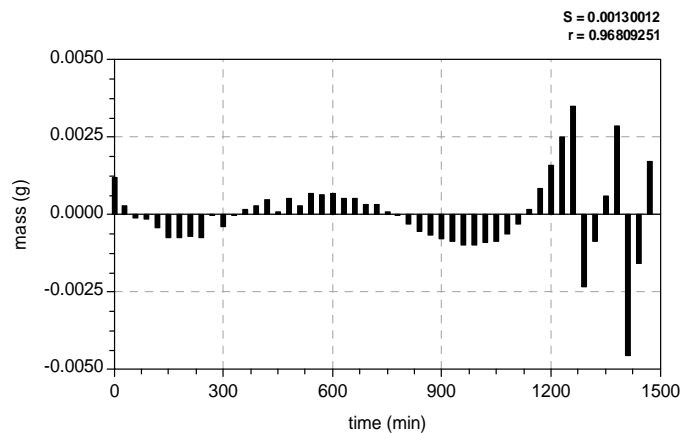


Fig.17. The graph of error in the model (1)

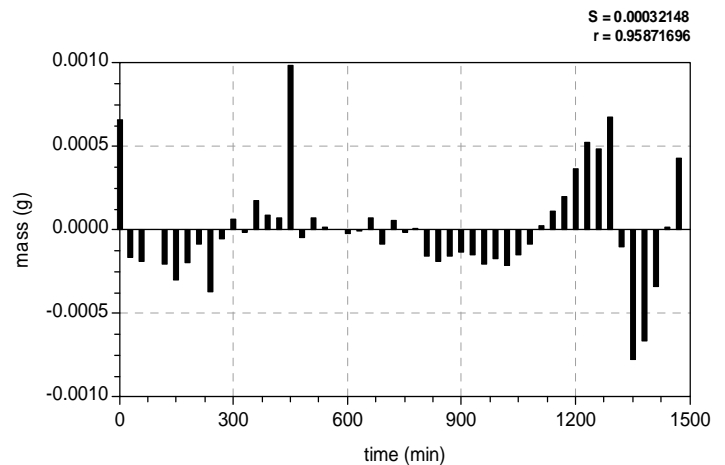


Fig.18. The graph of error in model (2)

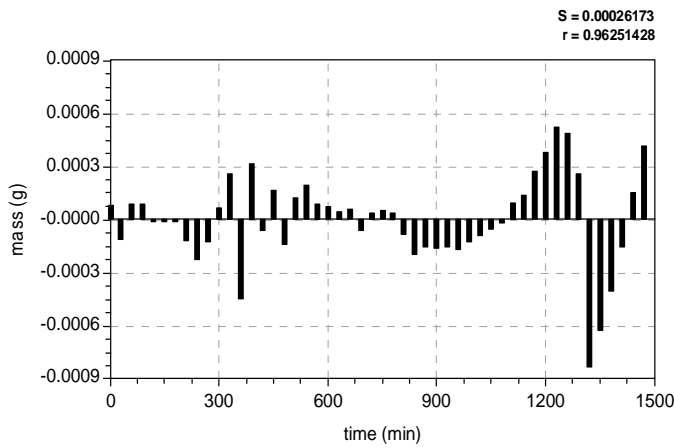


Fig.19. The graph of error in model (3)

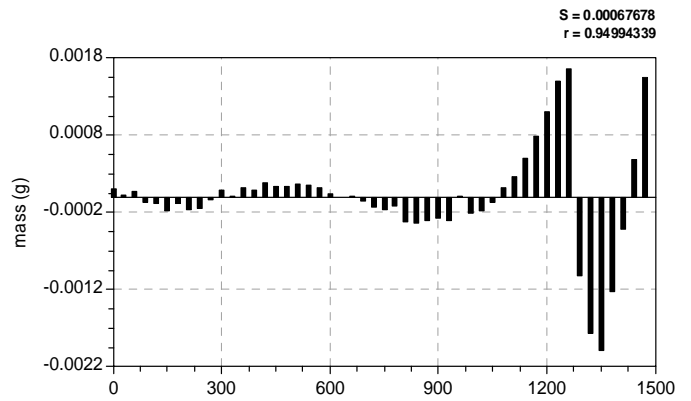


Fig.22. The graph of error in model (6)

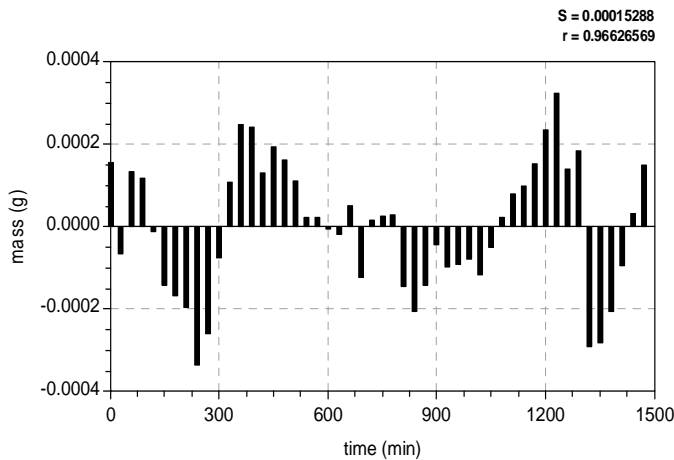


Fig.20. The graph of error in model (4)

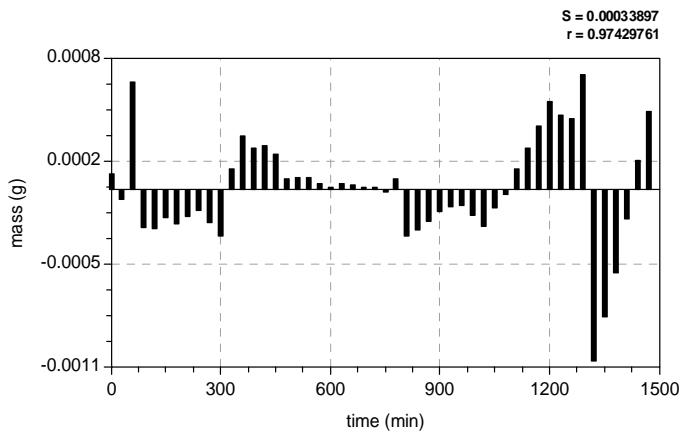


Fig.21. The graph of error in model (5)

The Jarque – Bera test always employs the values g_1 and b_2 respectively to represent the skewness and kurtosis of a distribution.

The chi-square value computed is always evaluated with two degrees of freedom:

$$\chi^2 = n \left[\frac{g_1^2}{6} + \frac{(b_2 - 3)^2}{24} \right].$$

At the significance level $\alpha = 0.05$, the normality hypothesis is accepted if the value χ^2 calculated is less than the tabled critical value of the chi-square function with two degree of freedom, $\chi_{0.05}^2(2) = 5.99$. [25]

In our case the normality hypothesis was accepted for the residuals in models (1) - (6).

For example, the values of χ^2 for the errors in the models (5) and (6) were respectively 2.99 and 3.88.

The histograms of errors in the models (4) and (5) together with the theoretical Gaussian curves are given in Figs. 23 – 24.

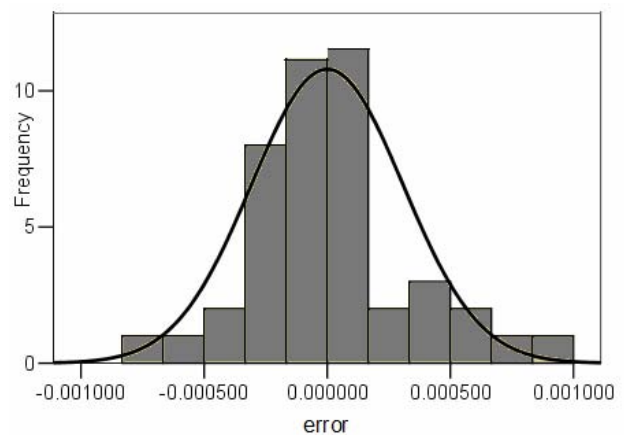


Fig.23. Errors' histogram in model (4)

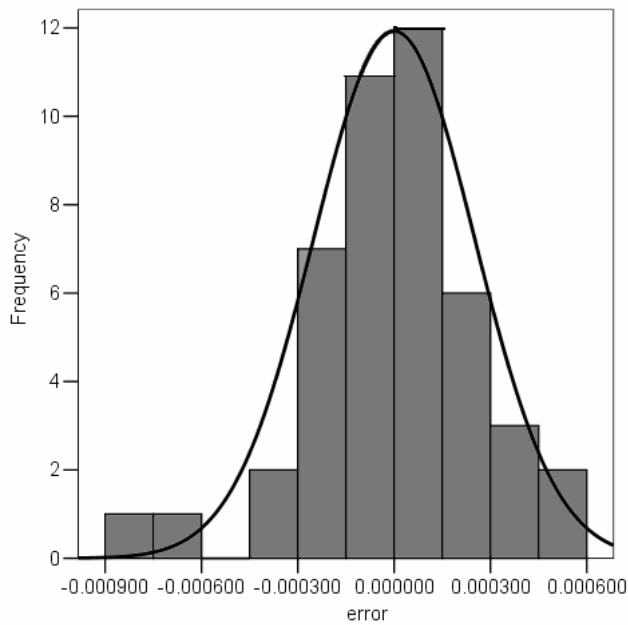


Fig.24. Errors' histogram in model (5)

The quantile – quantile diagram (Q-Q plot) is a method that compares the ordered values of the observed variable with the quantile values of theoretical specified distribution (in our case, the normal distribution).

If the tested variable's distribution is normal, then the Q - Q points describe a straight line that is superposed with the line that represents the theoretical distribution, e.g. passes through zero and its shape is one.

Figs. 25 – 26 represent the Q – Q plots of errors in models (5) and (6).

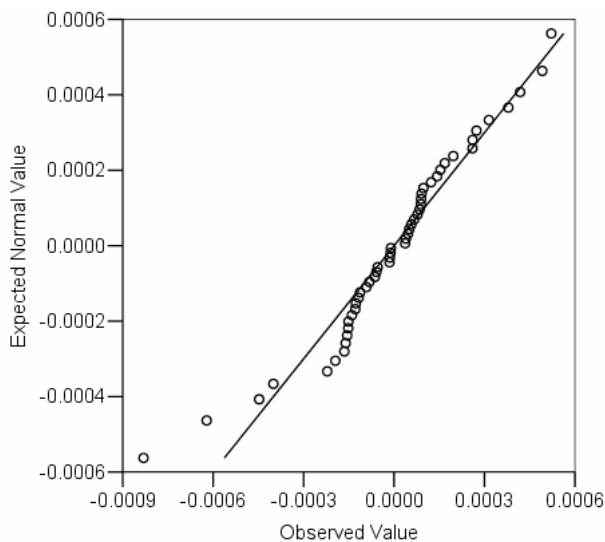


Fig.25. Q-Q plot for errors in model (5)

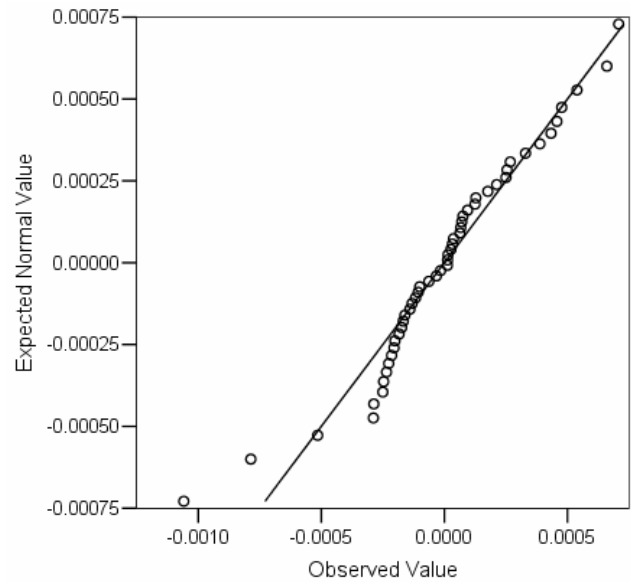


Fig.26. Q-Q plot for errors in model (6)

The results of Jarque - Bera test, the histograms and Q-Q plots' analysis lead us to accept the hypotheses that all the residuals are normally distributed.

In order to verify the residual correlation, the autocorrelation function is used.

We remember the following definitions:

The autocorrelation function of a discrete process $(X_t, t \in \mathbf{Z})$ is defined by:

$$\rho(h) = \frac{Cov(X_t, X_{t+h})}{\sqrt{D^2(X_t)D^2(X_{t+h})}}, h \in \mathbf{Z},$$

where:

$D^2(X_t)$ is the variance of the variable X_t ;

$Cov(X_t, X_{t+h})$ - the covariance of X_t and X_{t+h} .

Since, practically we work with realizations of a process $(X_t, t \in \mathbf{Z})$, an estimation of autocorrelation function is the empirical autocorrelation function, ACF, defined by:

$$\hat{\rho}(h) = \frac{\sum_{t=1}^{n-h} (x_t - \bar{x})(x_{t+h} - \bar{x})}{\sum_{t=1}^n (x_t - \bar{x})^2},$$

where:

- x_t is a realization of X_t ,

- \bar{x} - the arithmetic mean of x_1, \dots, x_n ,

- h - the lag.

In Figs. 27 and 28 the ACF of errors in the models (5) and (7) are represented. It can be seen that the values of ACF are inside the limits of the confidence interval at the confidence level of 95%.

So, we can admit accept the hypothesis that the residuals are uncorrelated.

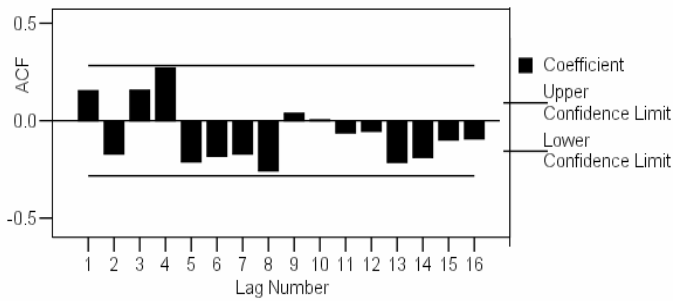


Fig.27. ACF of errors in model (5)

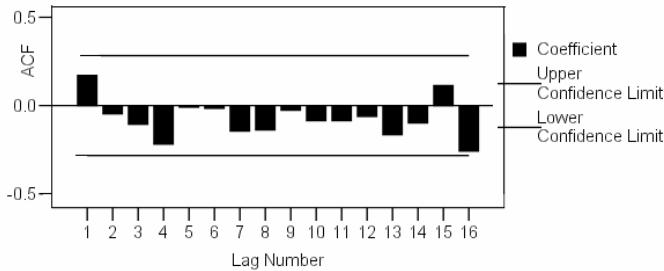


Fig.28. ACF of errors in model (6)

The test Bartlett is used to verify the homoscedasticity hypothesis of the errors, i.e.

H_0 : the errors have the same variance.

To do it, the selection values were divided in $i = 3$ groups, with $n_1 = n_2 = 16$ data and $n_3 = 17$ data.

Let us denote by s_1^2, s_2^2, s_3^2 the selection variances of the groups, s^2 - the selection variance of the sample and:

$$X^2 = \frac{-\sum_{j=1}^i n_j \ln \frac{s_j^2}{s^2}}{1 + \frac{1}{i-1} \sum_{j=1}^i \left(\frac{1}{n_j} - \frac{1}{n} \right)}$$

The hypothesis H_0 is accepted if X^2 calculated is less than $\chi_{0.05}^2(2)$. [26]

This condition was satisfied for the residuals in the models (1) – (6). For example, for the model 5, $X^2 = 4.848$.

The tests' conclusions are: the residuals are normally distributed, uncorrelated and homoscedastic, so the models describe very well the erosion – corrosion evolution in time.

The absolute mass variation function with respect to time (Fig.29) and the absolute mass loss on time surface (Fig.30) were also determined.

Taking into account the last values calculated, corrosion speeds were also calculated.

For the samples 5 and 6 the values are respectively 0.31 mm per year and 0.46 mm per year.

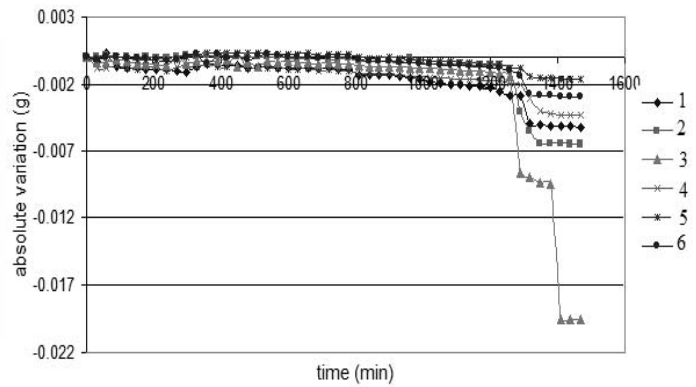


Fig.29. The graph of absolute mass loss variation

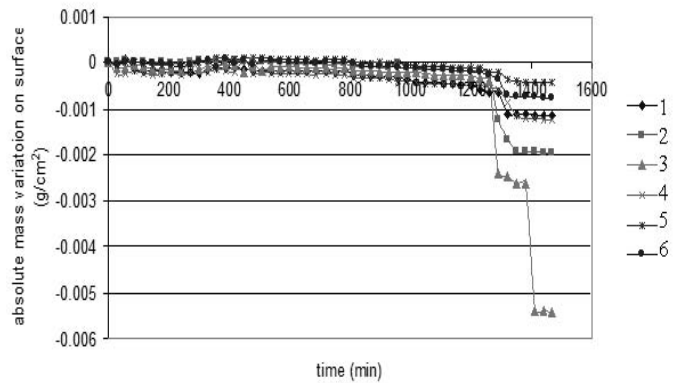


Fig.30. The graph of absolute mass loss on surface

V. CONCLUSIONS

In this article the results of studies on some copper - base composites corrosion on saline media were presented. Comparing their corrosion behavior we can conclude that:

- The samples were resistant at general corrosion in the studied media.
- The pitting test proves that the materials are not exposed at this corrosion type.
- The composites impregnated were less resistant to the corrosion comparing to the non - impregnated one, in both situation (the presence and the cavitation absence).
- The cavitation presence accentuates the corrosion speed.
- The mass loss of material in cavitation field, function of time can be described by a polynomial of 4th degree, for all composites, and the mathematical models found are good point of view of statistic, since the coefficients are significant and the residuals are independent, homoscedastic and normally distributed.

These results are concordant with the studies previously done on other materials of the same type [26] – [27].

REFERENCES

[1] S.M. Abd El Halem and E.E. Abd El Aal, "Electrochemical Behavior of Copper in Alkaline-Sulfide Solutions", *Corrosion*, vol.2, no.2, pp.121-128, 2006.

[2] G. Grechanyuk, V.A. Denisenko and L. Orac, "Structure and corrosive firmness of composition materials on basis of copper and molybdenum electron beam technology method", *Annals of "Dunarea de Jos" University of Galati, Metallurgy and Materials Science, Fasc. IX*, vol. 1, 2007, to be

published.

- [3] V. G. Grechanyuk, V.A. Denisenko and L. Orac, "Studies and research on mechanical properties and the influence of structural defects for the Cu-Mo composite materials obtained using the PVD metod", *Proceedings of 2nd International Workshop in Geoenvironment and Geotechnics, Milos Island, Greece*, 2008, pp.237-243.
- [4] J. Jankowski, "Electrochemical methods for corrosion rate determination under cathodic polarisation conditions – A review. Part I – DC Methods", *Corrosion reviews*, vol.20, no.3, pp.159 – 177, 2002.
- [5] http://en.wikipedia.org/wiki/Electron_microscope
- [6] V.- P. Păun, C. Udriște, C. Pătrășcoiu, "On the Erosion Process of the Ductile Materials", in *Mathematical methods, computational techniques, non-linear systems, intelligent systems, Proceedings of MAMECTIS'08, NOLASC'08, WAMUS'08*, pp. 256 – 263, 2008.
- [7] I. Kovacs, I. Andras, M. S. Nan, F. D. Popescu, "Theoretical and experimental Research Regarding the determination of Non-Homogenous Material mechanical Cutting characteristics", in *Simulation, Modelling and Optimization, Proceedings of the 8th WSEAS International Conference on Simulation, Modelling and Optimization '08* pp.232-237, 2008.
- [8] H. T. Huynh, J. - J. Kim, Y. Won, "Comparison of Nonlinear Methods for hematocrit Estimation from the Transduced Anodic Current Curve", in *Mathematical methods, computational techniques, non-linear systems, intelligent systems, Proceedings of MAMECTIS'08, NOLASC'08, WAMUS'08*, pp. 156 – 161, 2008.
- [9] <http://www.radiometer-analytical.com/pdf/voltalab>
- [10] R.T. Knapp, J.W. Daily, F.G.Hammit, *Cavitation*, Mc Graw-Hill, 1970, pp.25 – 30.
- [11] M. Hodnett, M.J. Choi, B. Zequiri, "Towards a reference ultrasonic cavitation vessel. Part I: preliminary investigation of the acoustic field distribution in a 25 kHz cylindrical cell", *Ultrasonic. Sonochemistry*, vol.14, pp.29 – 40, 2007.
- [12] H. G. Flynn, "Physics of acoustic cavitation in liquids", in: *Physical Acoustics*, vol. 1 (part B), W.P.Mason (Ed.), Academic Press, pp.57-172, 1964.
- [13] R. Apfel, "Sonic effervescence: a tutorial on acoustic cavitation", *J. Acoust. Soc. Am.*, vol. 101, pp.1227-1237, 1997.
- [14] E. A. Neppiras, *Acoustic cavitation*, Phys. Rep., vol.61, pp. 159-251, 1980.
- [15] T.G. Leighton, *The Acoustic Bubble*, Academic Press, London, 1994, Chapter 3.
- [16] A. Weissler, "Sonochemistry: the production of chemical changes with sound waves", *J. Acoust. Soc. Am*, vol.25, no.4, pp.651-657, 1953.
- [17] A. Thiem, K. Nickel, U. Neis, "The use of ultrasound to accelerate the anaerobic digestion of sewage sludge", *Water Sci. Technol.*, vol.36, pp.121-128, 1997.
- [18] R.A. Rory, "Physical aspects of sonoluminescence from acoustic cavitation", *Ultrasonic, Sonochemistry*, vol.1, no.1, pp. S5 - S8, 1994.
- [19] C. S. Dumitriu and A. Barbulescu, *Studies concerning the copper base alloys used in naval constructions – Modeling the mass loss in different media*, Sitech, Craiova, 2007, pp.70 – 71.
- [20] A. Barbulescu, V. Marza, "Electrical effect induced at the boundary of an acoustic cavitation zone", *Acta Physica Polonica B*, vol.37, no. 2 pp. 507-518, 2006.
- [21] A. Barbulescu, "Models of the voltage induced by cavitation in hydrocarbons", *Acta Physica Polonica B*, vol. 37, no.10, pp.2919-2931, 2006.
- [22] T. Shimamura, J. Yamauchi, "Spectral Substraction with Non-Stationary Noise estimation utilizing Harmonic Structure", in *Proceedings of the 4th WSEAS International Conference on Electronics, Control and Signal Processing*, pp.47-52, 2005.
- [23] M. F. M. Zain, S. M. Abd, K. Sopian, M. Jamil., A. I. Che-Ani, "Mathematical regression Model for Prediction of Concrete Strength", in *Mathematical methods, computational techniques, non-linear systems, intelligent systems, Proceedings of MAMECTIS'08, NOLASC'08, WAMUS'08*, pp. 396 – 420, 2008.
- [24] R. Bourbonais, *Econometrie*, Dunod, Paris, pp.54 - 78
- [25] D. Seskin, *Handbook of parametric and nonparametric statistical procedures*, Chapman and Hall, 2007, pp. 219 – 220
- [26] A. Bărbulescu, C. Koncsag, "A new estimation model of the mass transfer coefficients at the ethanethiol extraction with alkaline solutions in packed columns", *Applied Mathematical Modelling*, vol.31, no.11, pp. 2515 – 2523, nov. 2007
- [27] A. Barbulescu and C.S. Dumitriu, "Models of the mass loss of some copper alloys", *Chem. Bull. Politehnica University (Timișoara)*, vol. 52 (66), nos. 1 - 2, pp. 120-123, 2007.
- [28] A. Barbulescu, D.-C. Toncu, "Copper-Base Materials For Shipbuilding – Corrosion Behaviour", *Chem. Bull. Politehnica University (Timișoara)*, to be published